Theor Chem Acc (2004) 111:303–310
DOI 10.1007/s00214-003-0536-1

Theoretical
Chemistry Accounts

Regular article

A possible role of histidine residues in long-range electron transfer in proteins

Mariangela Di Donato, Andrea Peluso

Dipartimento di Chimica, Università di Salerno, 84081 Baronissi, Salerno, Italy

Received: 17 January 2003 / Accepted: 30 April 2003 / Published online: 30 January 2004

Abstract. Metal–histidine complexes are recurrent structural motifs in proteins exhibiting long-range electron transfer (ET), being involved both as electron donor or acceptor groups and as bridges which mediate ET between other cofactors. That observation suggests that the histidine residue could play an active role in ET, beyond that of simply binding the metal ion. Density functional theory and ab initio computations, performed on a simplified model system of the ET chain in semisynthetic Zinc cytochromes, confirm that expectation, suggesting that the nitrogen site of the histidine ring can exchange both a proton and a whole hydrogen atom with its redox partners. This finoling indicates that proton-assisted ET appears to be a plausible mechanism in this system.

Keywords: Electron transfer – Proton-assisted electron transfer – Ruthenium complexes – Histidine residues – Density functional theory computations

1 Introduction

The high efficiency and specificity of long-range electron transfer (ET) in biochemical systems is certainly strongly related to their structural features. Recent developments in high-resolution X-ray diffraction and spectroscopy have just opened the way towards the understanding of the structure – property relationships in such biosystems [1, 2, 3], a key step for achieving one of the major objective research pursuits nowadays: designing molecular machines which are able to reproduce the functions and efficiency of their biochemical counterparts [4, 5, 6, 7].

ET proteins have very complicated structures, but, in spite of their complexity, they exhibit many common features, such as the presence of metal centres, which are usually coordinated to one or more histidine residues of the protein backbone or to porphyrin rings. Iron ions are usually coordinated to porphyrin rings, as in the heme group, but in photosynthetic reaction centres (RCs) the two most important redox cofactors, the primary and secondary quinone, are linked together by a bridge constituted by a non-heme iron ion, Fe(II), coordinated to four histidine residues [8]. Different metals, such as copper or nickel, are usually coordinated to amino acid residues, especially to histidine. Metal–histidine complexes are the redox sites in azurin and plastocyanines, where a single copper–histidine complex is present [9, 10], and in cytochrome oxidase, where a binuclear copper site acts as an intermediate for long-range ET from an external cytochrome c group to the iron ion of the hemeA3 group, the site where the reduction of oxygen to water occurs [11]. Finally, Ni–Fe hydrogenases, which catalyse the reversible oxidation of molecular hydrogen, contain a single Ni–Fe active site, with the Ni ion coordinated to four cysteine residues and to an additional ligand, tentatively assigned as a μ-oxo species [12].

In this paper we focus our attention on such metal–histidine complexes, in the attempt to understand if there are structural features which make them particularly suitable for long-range ET. The histidine residue could, in fact, play an important role in long-range ET, because its N–H group can be involved in acid–base equilibria, with the effect that protonation or deprotonation of the histidine nitrogen not coordinated to the metal ion could stabilize different redox states of the latter.

To better substantiate this concept, let us consider a metal cation M with two stable oxidation states, M(II) and M(III). Let us assume that in the M(II) oxidation state the chemical bond between M and the histidine nitrogen can be represented as a usual dative bond, with the nitrogen lone pair shared by the two nuclei and one unpaired electron localized on the d orbitals of M, structure I of Scheme 1. Under particular circumstances, i.e. an electric field created by oxidation or reduction of a molecule close to the metal complex, the unpaired electron could also be localized on the imidazole ring, giving the metastable electronic structure II which can

Contribution to Jacopo Tomasi Honorary Issue

Correspondence to: A. Peluso
e-mail: apeluso@chem.unisa.it

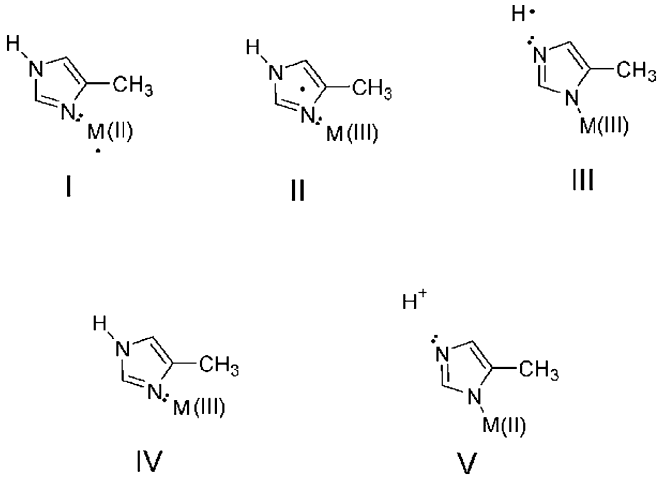

Scheme 1.

evolve into structure III by releasing a hydrogen atom. The effect of this electronic rearrangement is the oxidation of the metal ion and the formation of a hydrogen atom, which can then reduce another redox centre of the protein. Hydrogen-atom shifts are in fact common processes in the chemistry of radicals, exhibiting low energy barriers [13]. The reason why such a process could be favoured in proteins rests on the fact that the electrostatic charge of the metal complex is not varied upon oxidation, so the process can occur without involving the slower motions of counterions. As a matter of the fact, many redox reactions in proteins require small solvent reorganization energies [14, 15, 16].

On the other hand, one can envision that the N–H group of the histidine ring can neutralize negative charges produced by redox processes involving neighbouring groups, hydrogen-bonded to the histidine ring. That can, for instance, occur if the stablest electronic configuration of the metal–histidine complex is that of structure IV, with the dative bond formed when the metal ion has a formal oxidation state +3. The release of a proton can lead to electronic rearrangement towards structure V, in which the metal ion is formally +2, so that even though ET has not yet taken place – the process IV→V is a charge transfer from histidine to metal – the complex already has the electronic configuration of the reduced form, for instance a lower ionization potential, and is therefore able to release an electron to another redox centre. In the latter case, the metal–histidine complex acts as a bridge for ET between two redox cofactors, as shown in Scheme 2:

$$
\begin{array}{l}
A^- \cdots \text{H-His-M}^{3+}\ B \\
\qquad\downarrow \\
\text{A-H} \cdots \text{His-M}^{2+}\text{B} \\
\qquad\downarrow \\
\text{A-H} \cdots \text{His-M}^{3+}\ B^- \\
\qquad\downarrow \\
\text{A} \cdots \text{H-His-M}^{3+}\text{B}^-
\end{array}
$$

Scheme 2.

In order to apply these concepts to concrete examples, let us consider two cases in which metal–histidine complexes act as bridges for long-range ET: the bacterial photosynthetic RC and the cytochrome oxidase. In the former system, two redox cofactors, the primary (Q_A) and the secondary quinone (Q_B), are held together by a bridge constituted by an iron ion (Fe^{2+}) coordinated to four histidine and one glutamic residues. Two histidine residues are hydrogen-bonded to Q_A and Q_B, so that a continuous chain of hydrogen bonds connects Q_A to Q_B, through the metal–histidine complex [8]. Theoretical studies have shown that ET from Q_A^- to Q_B can occur via a proton-assisted ET (PAET) mechanism, consisting of an initial shift of the hydrogen-bonded histidine proton towards the oxygen of Q_A^-, followed by a double hydrogen-atom transfer in the opposite direction. The latter step causes the reduction of Q_B to neutral semiquinone and the simultaneous oxidation of Q_A–H to quinone (Scheme 3) [17].

$$
\begin{array}{l}
Q_A^- \cdots \text{H-His-Fe-His-H} \cdots Q_B \\
\quad \rightarrow Q_A\text{-H} \cdots {}^-\text{His-Fe-His-H} \cdots Q_B \\
Q_A\text{-H} \cdots {}^-\text{His-Fe-His-H} \cdots Q_B \\
\quad \rightarrow Q_A \cdots \text{H-His-Fe-His}^- \cdots \text{H-}Q_B \\
Q_A \cdots \text{H-His-Fe-His}^- \cdots \text{H-}Q_B \\
\quad \rightarrow Q_A \cdots \text{H-His-Fe-His-H} \cdots Q_{B^-}
\end{array}
$$

Scheme 3.

In the somewhat unusual ET mechanism illustrated in Scheme 3, the electron carriers are whole hydrogen atoms, which, by shifting their positions between the two possible hydrogen-bond equilibrium sites in the hydrogen-bond chain connecting the two redox cofactors, bring an electron from one end of the chain to the other, without localizing it on the higher-energy state of the bridge. That is possible if the electronic structure of the metal complex can rapidly switch from form I to III of Scheme 1, when a suitable perturbation, the arrival of an additional electron on one end of the hydrogen-bonded chain, is turned on.

As already mentioned, another example of a metal–histidine complex which acts as a bridge for ET is provided by the binuclear Cu_A complex of cytochrome c oxidase. That is a mixed-valence complex Cu(I)–Cu(II), in which the two copper ions, held together by a bridge of two sulphur atoms, are both coordinated to histidine residues, (Fig. 1). The binuclear complex is connected to its redox partner, a bis-histidine iron heme, by a network of hydrogen-bonds, which involves the histidine of the binuclear copper complex, a peptide linkage and one of the two carboxylate groups of the iron heme [11]. In that case, the additional electron released by a cytochrome c to Cu_A could be localized on the histidine ring, as in structure II of Scheme 1, thus promoting the release of a whole hydrogen atom, which could then reduce the iron heme. Indeed, Fourier transform IR difference spectra have shown that the carboxylic group of the heme group is partially protonated upon ET from Cu_A [18].

Ruthenium–histidine complexes have been widely used as redox centres for studying ET paths in semisynthetic

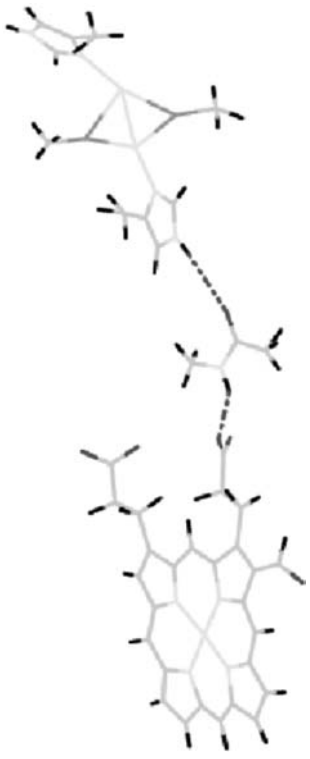

Fig. 1. The hydrogen bonded chain connecting the Cu_A and $heme_A$ cofactors in cytochrome c oxidase. From protein databank, entry 1OCC

ET proteins. Among the various semisynthetic ET proteins reported in the literature [19, 20, 21], one of the most studied is a Zinc cytochrome c modified with the introduction of a pentaamino complex of Ru(III). The metal ion can be coordinated to several histidine residues, so suitable complexation of different protein sites is a practical route to study, without changing the nature of the electron donor and acceptor pair, how ET rates depend both on the distance between the two redox partners and on the molecular structure of the interposed bridge [22].

In Zinc cytochrome c, the electron donor group is a Zinc porphyrin cofactor, which, upon excitation to its first triplet state, transfers one electron to the Ru–histidine complex. The kinetics of ET has been studied by means of a flash–quench technique: the reduced ruthenium complex is excited with a laser pulse in a high-energy electronic state, from which the excited electron (4*d*) is quickly removed by a strong electron acceptor, leaving a hole in the t_{2g} shell of the Ru ion. The subsequent excitation of the Zinc porphyrin promotes ET from the excited macrocycle to Ru(III); ET can then be monitored by recording the absorption spectrum of the ruthenium complex as a function of time. The ET step and the charge-recombination process which follows ET both occur in microseconds [23, 24].

It is worth noting that, at least in the case in which the ruthenium complex is coordinated to His39, there is a continuous chain of hydrogen bonds which connects the two redox centres. In fact, the X-ray structure of cytochrome c has shown that His39 is connected to the Zinc heme cofactor by a chain of hydrogen bonds involving Gly41, whose peptide nitrogen is at a hydrogen-bond distance from one of the propionate groups of the heme molecule, Ser40, and a structural water molecule [25]. The hydrogen-bond chain is reported in Scheme 4.

$$\text{Heme-COO}^{-}\cdots\text{HN-CHO}\cdots\text{HO-R}^{\text{Ser40}}\cdots\text{HOH}\cdots\text{HIm}^{\text{His39}}\text{-Ru}$$

Scheme 4.

It is therefore of interest to clarify if proton and/or hydrogen atom shifts along the hydrogen-bond chain can assist long-range ET in such a system, where the ET path involves at least one peptide linkage, together with hydrogen bonds formed by the side chains of specific amino acids. With that purpose in mind, we will first analyse the electronic structures of $[Ru(NH_3)_5ImH]^{n+}$ ($n = 2,3$) complexes, focussing attention on the influence of metal coordination on the histidine acid–base properties. Then we will consider the effect of a perturbation, i.e. the arrival of an additional electron on a group close to the ruthenium complex, by considering a model system constituted by $[Ru(NH_3)_5ImH]^{3+}$ and a semiquinone molecule held together by a hydrogen-bond chain involving a peptide linkage.

2 Electronic structure of ruthenium–imidazole complexes

The geometries of complexes $[Ru(NH_3)_5ImH]^{n+}$, $n = 2, 3$, and $[Ru(NH_3)_5Im]^{2+}$ were fully optimized by using the Becke three-parameter hybrid potential with the Lee, Yang and Parr correlation functional (B3LYP)/density functional theory (DFT) method and the standard 3-21g* basis set, for both Ru(II) and Ru(III) oxidation states. Wherever not specified all the computations were carried out with that basis set. All the computations were performed with the G94 package [26]. Open-shell systems were studied at the unrestricted Hartree–Fock (UHF) level of theory.

In analogy with electron paramagnetic resonance (EPR) studies [27], we adopted a coordinate frame with the *z*-axis directed along the NH_3–Ru–Im axis and the *x*- and *y*-axes rotated by 45° with respect to the other two metal–ligand axes.

The Ru(III) complex is an open-shell system, for which more electronic configurations are possible. Here we considered only the doublet state, which according to the EPR results is the ground state of the complex [27]. Selected geometrical parameters of the optimized structures of $[Ru(NH_3)_5ImH]^{n+}$, $n = 2, 3$, and $[Ru(NH_3)_5Im]^{2+}$ are reported in Table 1 (for the atom numbering see Fig. 2).

In all the cases, the ruthenium complexes are approximately octahedral, with the imidazole ring being essentially planar, and oriented in a staggered conformation with respect to the four equatorial NH_3 ligands. All the computed metal–ligand distances are slightly longer if compared with the X-ray data, available only for the Ru(III) complex [27, 28, 29], but they are in line with the general trend observed in the crystal structure: the four Ru–NH_3 distances are all similar, but for that

Table 1. Computed and experimental bond distances (Å) for $[Ru(NH_3)_5ImH]^{n+}$, $n = 2, 3$, and $[Ru(NH_3)_5Im]^{2+}$ complexes. The X-ray and ab initio results are from Ref. [29]

	DFT/B3LYP/3-21g*			X-ray Ru(III)–Im–H	Ab initio Ru(III)–Im–H
	Ru(III)–ImH	Ru(II)–ImH	Ru(III)–Im		
$Ru–N_1$	2.06	2.10	1.98	2.02	1.99
$Ru–N_2$	2.19	2.20	2.19	2.07	2.15
$Ru–N_3$	2.19	2.20	2.20	2.07	2.15
$Ru–N_4$	2.22	2.10	2.20	2.11	2.18
$Ru–N_5$	2.20	2.20	2.19	2.12	2.15
$Ru–N_6$	2.20	2.20	2.19	2.07	2.25
$N_1–C_1$	1.36	1.34	1.45	1.31	
$N_1–C_2$	1.41	1.41	1.39	1.41	
$C_1–N_7$	1.34	1.37	1.31	1.31	
$N_7–C_3$	1.41	1.39	1.43	1.39	
$C_3–C_2$	1.37	1.38	1.39	1.34	

between the metal ion and the ammonia nitrogen opposite the imidazole ring, which is slightly longer [29]. The $Ru–N_1$ distance is significantly shorter than the other ones. The experimental metal–ligand distances are reported in Table 1, together with the results of DFT computations and the results of an ab initio computation available in the literature [29].

The oxidation state of the metal has little influence on the Ru–N distances, but for a slight variation in the $Ru–N_1$ and $Ru–N_4$ ones, which are, respectively, 0.042 Å longer and 0.12 Å shorter for the Ru(II) complex than for the Ru(III) one (Table 1). In the case of Ru(II), the complex has an axially distorted octhaedral coordination, whereas in the Ru(III) complex only the distance between the imidazole ligand and the metal is significantly shorter than the other ones, thus suggesting the existence of significant interactions between Ru(III) and the histidine ligand. That could reflect a partial distortion of the octhaedral coordination upon the arrival of one electron on the metal, value to the increased electronic repulsion between ligands and metal. The electronic structure of the two complexes is quite different and that significantly affects the geometry of the imidazole ring (Table 1). For the Ru(II) complex, where the metal ion has a closed-shell electronic structure, with a completely filled t_{2g} shell lying at significant lower energy than the empty π orbitals of the imidazole ring, the molecular orbitals (MOs) are essentially localized either on the metal or on the imidazole ligand, the extent of electron delocalization between orbitals of the two moieties being quite low. In contrast, for the Ru(III) complex there are significant interactions between the *d* orbitals of the metal and the π MOs of the imidazole ring and that causes significant changes of the bond lengths of the imidazole ring. Inspection of Fig. 3, where the π MOs of the imidazole ligand are reported for both complexes, shows that they are quite different in the two metal oxidation states; while for Ru(II) they are very similar to what is expected for an isolated imidazole ring, with bonding interactions prevalently localized between the $N_1–C_1$ and $C_2–C_3$ pair, as expected if structure I of Scheme 1 predominates over all others, in the case of Ru(III) there are significant bonding interactions between

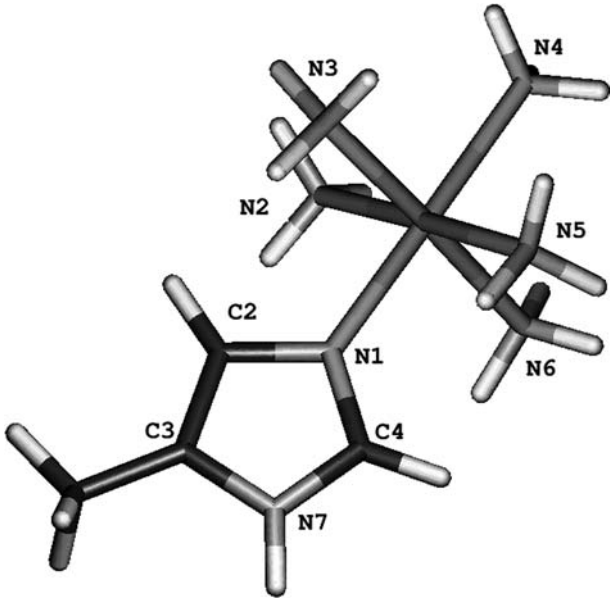

Fig. 2. Atom numbering and optimized geometry of $[Ru(NH_3)_5ImH.^{2+}]$

C_1 and N_7, and between N_1 and C_2, thus suggesting that structure V of Scheme 1 can play a role. Accordingly, the bond $C_1–N_7$ distance is significantly shorter for the Ru(III) complex than for the Ru(II) one, in line with experimental results, and the $N_1–C_2$ one is longer in the former complex with respect to the latter (Table 1).

All these observations show that in the case of Ru(III) a partial ligand-to-metal charge transfer from a π orbital of the imidazole towards an empty t_{2g} orbital of the metal takes place. In fact, even though the EPR analysis has shown that the unpaired electron is completely localized on the metal, which carries 0.98 of the total spin density, and that finding is in agreement with the results of our computations, which yields a spin density at the metal site of 0.94, the additional positive charge on the metal ion lowers the energy of the occupied t_{2g} orbitals, which are now close in energy to the π orbitals of the imidazole ring and can then interact with

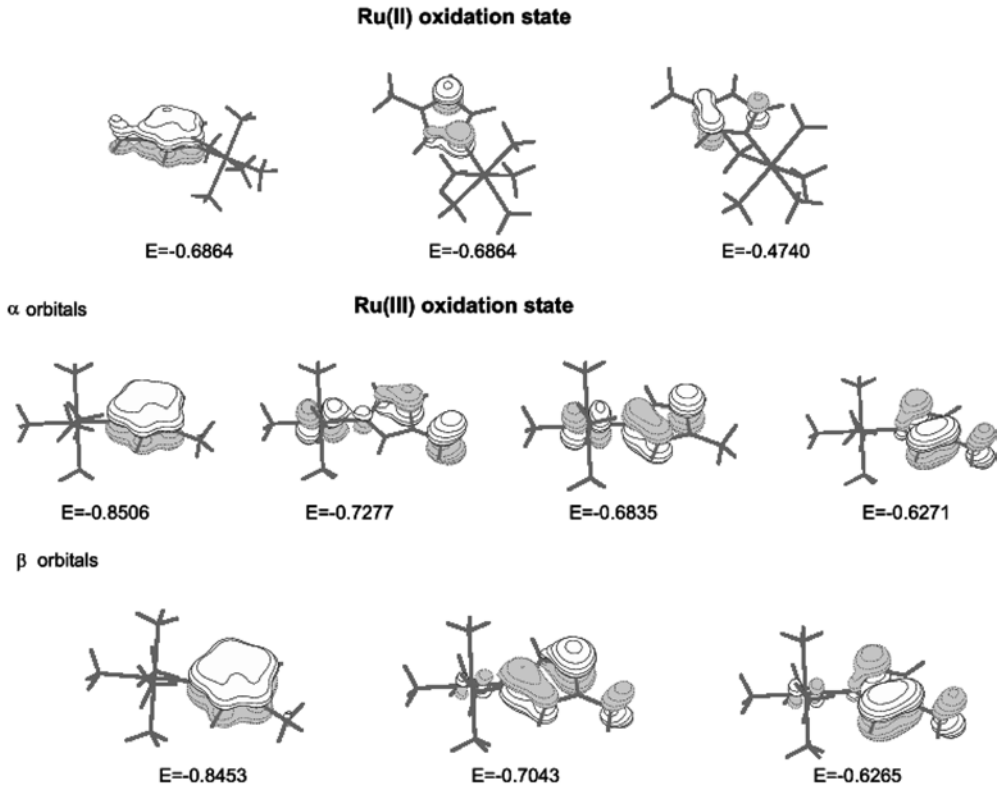

Fig. 3. Occupied imidazole π molecular orbitals of $[Ru(NH_3)_5ImH]^{n+}$, $n = 2, 3$

Table 2. Ionization potentials, N–H homolytic and heterolytic dissociation energies (gas phase) and reduction potential (water solution, volts) of $[Ru(NH_3)_5ImH]^{n+}$, $n = 2, 3$. All energies in electronvolts

	Ru(III)	Ru(II)
Ionization potential	–	13.270
Reduction potential	0.16	–
D_{NH} heterolytic	5.356	9.648
D_{NH} homolytic	6.059	5.092

them. Mulliken population analysis yields a net positive charge on the imidazole moiety significantly larger than those on the ammonia ligands (0.52 versus 0.38) for the Ru(III) complex, whereas for the Ru(II) complex it is slightly lower (0.23 versus 0.29).

A suitable benchmark property which allows us to verify the reliability of the present computations is provided by the reduction potential of $[Ru(NH_3)_5ImH]^{3+}$. The computed ionization potential of $[Ru(NH_3)_5ImH]^{2+}$ in the gas phase is 13.3 eV (Table 2). In order to compare it with the experimental reduction potential measured in aqueous solution, which is of the order of 0.15–0.12 V versus the normal hydrogen electrode (NHE) [27, 28, 30], solvent effects have to be taken into account. The latter ones can be reliably modelled by using Tomasi's polarizable continuum model (PCM) method [31]. The computed relative energies of the complexes in the gas phase and in water are reported in Table 3. The ionization potential of the Ru(II) complex in water, computed at the DFT/B3LYP/PCM level is 4.64 eV. The reduction potential versus the NHE can then be obtained by using the following equation [32]:

$$E^0 = \mathrm{IP} - \lambda - E_{\mathrm{NHE}} \ , \qquad (1)$$

where IP is the ionization potential, λ is the total reorganization energy, including both the contribution deriving from solute–solvent interactions and from the

Table 3. Ab initio unrestricted Hartree – Fock/6–31 g relative energies and Mulliken's charges on Ru, imidazole, *N*-methylformamide (*br*) and semiquinone moieties for the intermediate states formed according to the proton assisted electron-transfer mechanism of Scheme 5. In the ab initio computation the basis set on the Ru atom is the standard 3–21 g

	ΔE (eV)	Charges (au)			
		Ru	Im	br	QH
Ru(III)-ImH···BrH···QH^-	0.0	1.706	0.137	−0.045	−0.886
Ru(III)-ImH···Br^-···HQH	0.300	1.705	0.137	−0.836	−0.074
Ru(II)-Im···HBr···HQH	−0.419	1.696	−0.649	−0.028	−0.021
Ru(II)-ImH···BrH···QH·	−2.12	1.399	0.0005	0.0084	0.034

relaxation of the molecular structure upon the removal of one electron, and E_{NHE} is the absolute reduction potential of the standard hydrogen electrode, i.e. 4.48 V [33].

As we referred to the adiabatic ionization potential rather than the vertical one, the contribution of the internal reorganization energy is already included in the relative energies reported in Table 3. The contribution of the solvent was estimated by single-point PCM calculations, neglecting geometry relaxations in solution, which are usually very small. The computed reduction potential of the complex is 0.16 V, in good agreement with the experimental results.

Since the principal aim of this work is to study the possibility that metal–histidine complexes could promote ET to a redox partner with a proton-assisted mechanism, it is important to examine the modifications in the electronic structure of these complexes induced by the deprotonation of the imidazole ligand. The most evident consequence of that process is a further mixing of the MOs between the metal centre and the imidazole ring, which causes a significant charge redistribution of the complex: in fact the negative charge on the imidazole is mostly transferred to the ruthenium ion, the residual charge on the ligand being only −0.102 au. In this case the spin density is not completely localized on the metal, which carries about half of it, the remaining part being distributed on the imidazole ligand. On the basis of these results it can be envisioned that the deprotonation of the imidazole favours an electronic redistribution of the complex that facilitates the reduction of the metal.

It is worth noting that the acid–base properties of the imidazole are strongly influenced by the coordination of a metal ion. The computed energy for extracting a proton from the nitrogen site of the imidazole ring is only 5.35 eV (Table 3), at the DFT/B3LYP/3-21g* level, when the imidazole is coordinated to $[Ru(NH_3)_5]^{3+}$, a very low value if compared with its counterpart for a free imidazole molecule in the gas phase, 16.04 eV, computed at the same level of theory, and for the Ru(II) complex, 9.65 eV. The reported results confirm that the pK_a of the imidazole ring of a histidine residue coordinated to a metal ion in a protein structure can be very different from the value measured in aqueous solution in the case of the free amino acid, and that the functional role of metal–histidine centres at the catalytic site of ET proteins is strongly correlated with the possibility of general acid–base catalysis by histidine residues induced by its augmented proton dissociability.

3 Long-range ET in a model system

In order to better clarify the role of the histidine proton in long-range ET, we have computationally analysed the plausibility of a PAET [17, 34, 38] in a model system, somewhat resembling the case of long-range ET from an excited Zinc heme to $[Ru(NH_3)_5ImH]^{3+}$ in semisynthetic Zinc cytochrome c. In such systems, at least when $[Ru(NH_3)_5]^{3+}$ is coordinated to His39, the X-ray structure has shown that the electron donor and acceptor groups are connected by a hydrogen-bond chain, which involves a peptide linkage, a hydroxyl group and a structural water molecule, in the sequence shown in scheme 4 [25]. In order to simplify computations we have replaced the Zinc heme group with a neutral semibenzoquinone (QH) and omitted both the hydroxyl group and the structural water molecule, since they are not expected to affect the energetics of the stationary states formed during the PAET processes. Water molecules and hydroxyl groups can exchange two protons or two hydrogen atoms in a concerted mechanism without changing their chemical structures, so their contribution to the energetics of the stationary states formed during the PAET process can be safely neglected. The case of a peptide linkage is different because after a double proton- or hydrogen-atom transfer the molecule undergoes isomerization from the stablest keto form to the enol one, which in the gas phase is predicted to be about 13 kcal/mol less stable than the keto form [34]. That is a significant contribution to the energy of the stationary states in which the enol form is present. Of course, the situation is different when the kinetics of the process is considered, because a concerted double transfer of protons or hydrogen atoms, required when a water or a hydroxyl group is present in the hydrogen-bond chain, could require a higher activation energy, but, since we are interested at the moment only in the energetics of the ET mechanism, water molecules have not been considered in the model system. The system we have adopted to model PAET in a semisynthetic ET protein is shown in Fig. 4.

The ET process which we are modelling here is basically different from that occurring in semisynthetic proteins; in the latter case ET is induced by the absorption of a photon by the heme group, whereas in the case we consider here ET from QH to Ru(III) is triggered by the arrival of an additional electron on the quinone. Furthermore, we assume that direct ET from the semiquinone anion to the Ru(III) complex via tunnelling is ruled out by the smallness of the electronic coupling term, so even though the ET process is highly exergonic, the electronic state $QH^{-}Ru^{3+}$ has a lifetime long enough to be detected.

The electron affinity of QH in the gas phase is much lower than that of $[Ru(NH_3)_5ImH]^{3+}$, so the initial state,

$$[Ru(NH_3)_5ImH]^{3+} \cdots HN\text{-}C = O \cdots QH^{-},$$

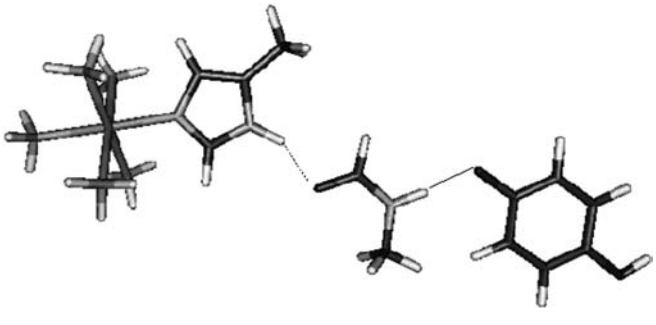

Fig. 4. The adopted model system for studying long-range electron transfer involving $[Ru(NH_3)_5ImH]^{3+}$ as an electron acceptor

is expected to be a highly excited state of the system. To estimate the energy of this state one can resort to two different approaches. The most direct one is that of using time-dependent (TD)/DFT [35] or multireference configuration interaction [36] methods to estimate the energies of the electronically excited states. On the other hand one can try to achieve self-consistency in an excited electronic state by using the minimum-energy geometries of the desired excited state and a suitable initial guess. In this paper both methods have been considered. While TD/DFT, performed with the Gaussian98 package, did not give any problems, converging to states with the desired electron densities, UHF/DFT always converged to the final state, i.e. that with the additional electron on the ruthenium atom. However, UHF ab initio computations performed by GAMESS package [37] yielded electronic states with the desired electron densities on each moiety, when performed on the appropriate geometries, with suitable initial guesses and inclusion of counterions around the ruthenium complex, placed in the same positions as observed in the X-ray structure [29]. The results of UHF ab initio computations and TD/DFT are very similar to each other; therefore, we discuss only those obtained at the TD/DFT level, ab initio results being summarized in Table 3, together with Mulliken charges for the molecular components of the model system of Fig. 4.

To better estimate energy differencies between the intermediate states formed in the PAET mechanism we expanded the basis set to 6–31 g for performing UHF ab initio computation, adding polarization functions on all the atoms engaged in hydrogen bonds. Although Mulliken's population analysis yields only a qualitative picture of the electronic distribution centred on nuclei, that is enough for our purposes, since we are only interested in the charges localized on a whole molecular moiety in the supramolecular aggregate.

In order to obtain the energy of the initial state, that with the additional electron wholly localized on QH, we performed a single-point TD/DFT computation on the model system of Fig. 4, using the optimized geometries of $[Ru(NH_3)_5ImH]^{3+}$, *N*-methylformamide and QH^-. As already mentioned, the ground state of the system exhibits the electronic configuration of $[Ru(NH_3)_5ImH]^{2+}$ and QH; the state with the additional electron wholly localized on QH is predicted by TD/DFT computation to be 3.7 eV higher in energy than the ground state and corresponds to a transition from a t_{2g} orbital of the ruthenium ion to the lowest unoccupied MO, which is an antibonding π level wholly localized on QH.

The first steps of PAET should consist of proton transfer from the N–H of the peptide bridge to QH^- or, alternatively, of a concerted double proton transfer from the N–H ligand to *N*-methylformamide and from the latter to QH^-. The single proton-transfer step is predicted to be slightly endergonic, around 0.1 eV, but, as already observed in previous works [34, 38], the energy difference is not high enough to rule out this step from the possible reaction paths. On the contrary the concerted transfer of the two protons lead to a intermediate state which is significantly at lower energy than the initial state (1.3 eV), so, even though the activation barrier for concerted proton transfer is expected to be higher, the high exergonicity of the process suggests that in this case the transition state would be located near the reactants, the so-called early transition state, so the energy barrier for the concerted double proton transfer is expected to be low.

As previously shown, when the imidazole ring releases a proton, a charge transfer from the imidazole ring to Ru(III) occurs, so the negative charge is no longer localized on the ligand, but it is mainly transferred to the metal centre, which is then reduced to Ru(II). The moieties forming the hydrogen-bond chain are now back in the neutral state, and the stablest nuclear configuration is restored by shifting back two whole hydrogen atoms, from the hydroxyl group to the imidazole nitrogen and from the quinone to the nitrogen of the peptide linkage, leading to the ET products. That step is also exergonic (2.35 eV) and yields the ET products in their ground state. The whole PAET mechanism is summarized in Scheme 5, together with the energy differences predicted by TD/DFT.

$$\text{Ru(III)-ImH}\cdots\text{BrH}\cdots\text{QH}^- \rightarrow \text{Ru(III)-ImH}\cdots\text{Br}^-\cdots\text{HQH} \quad \Delta E = 0.1\,\text{eV}$$

$$\text{Ru(III)-ImH}\cdots\text{Br}^-\cdots\text{HQH} \rightarrow \text{Ru(II)-Im}\cdots\text{HBr}\cdots\text{HQH} \quad \Delta E = -1.35\,\text{eV}$$

$$\text{Ru(II)-Im}\cdots\text{HBr}\cdots\text{HQH} \rightarrow \text{Ru(II)-ImH}\cdots\text{BrH}\cdots\text{QH} \quad \Delta E = -2.30\,\text{eV}$$

Scheme 5.

On the basis of the results, PAET appears to be a plausible alternative to direct ET via tunnelling.

4 Conclusions

The results reported in this paper show that the histidine ligand can play an active role in long-range ET involving metal–histidine complexes as a primary electron acceptor group. The nitrogen atom of the histidine ring not coordinated to the metal ion can in fact exchange both protons and hydrogen atoms with neighbouring groups, when a suitable perturbation, such as the arrival of an additional electron on a redox partner, is turned on. Moreover, computations have shown that one of the peculiar aspects of these complexes is the possibility of localizing an unpaired electron both on the metal ion and on the imidazole moiety, depending on the protonation state of the ligand. Thus, deprotonation of the imidazole ligand is strictly connected to reduction of the metal ion, induced by charge transfer from the ligand to metal. According to this finding, long-range ET in proteins where the metal–histidine complexes are connected to their redox partners by a hydrogen bond chain could occur by a proton-assisted mechanism, in which the electron carriers are whole hydrogen atoms, which migrate from the electron donor to the electron acceptor group along the hydrogen bond chain which connects them.

That alternative way of thinking about long-range ET in proteins appears particularly appealing in all those cases where the distance between the two redox partners is long enough to make the effective electronic coupling between them, the key parameter which regulates ET rates in all current theories [39, 40], extremely small, of the order of a few reciprocal centimetres. In those cases, the probability that ET occurred via tunnelling or superexchange mechanisms appears to be very low and alternative mechanisms are therefore needed [41]. PAET is fully compatible with the known chemistry of organic radicals [42], where hydrogen-atom transfers are known to occur easily, requiring small activation barriers, and it is also in line with recent results obtained for self-exchanges in iron bi-imidazoline complexes. In these complexes both the kinetics and thermodynamics suggest that the self-exchange reaction occurs by a net hydrogen-atom exchange reaction, rather than by stepwise mechanisms involving only proton transfer and/or ET [43].

Acknowledgements. It is a honour and also a great pleasure to dedicate this paper to Prof. Jacopo Tomasi as a sincere token of our esteem. We also thank the C.I.M.C.F., Department of Chemistry of the University Federico II of Naples (LSDM section) for providing computational facilities and the University of Salerno and MIUR (COFIN 2001) for financial support.

References

1. Feher G, Allen JP, Okamura MY, Rees DC (1989) Nature 339: 111
2. Bendall DS (1996) Protein electron transfer. Bios Scientific, Oxford
3. Lancaster GRD, Michel H (1996) In: Michel-Beyerle ME (ed) The reaction center of photosynthetic bacteria: structure and dynamics. Springer, Berlin Heidelberg New York, pp 23–35
4. Kilsa K, Kajanus J, Macpherson AN, Martensson J, Albinsson B (2001) J Am Chem Soc 123: 3069
5. Macpherson A, Liddel PA, Lin S, Noss L, Seely GR, DeGraziano JM, Moore AL, Moore TA, Gust D (1995) J Am Chem Soc 117: 7202
6. Sun L, Berglund H, Davydov R, Norrby T, Hammarstrom L, Korall P, Borje A, Philouze C, Berg K, Tran A, Andersson M, Stenhagen G, Martensson J, Almgren M, Styring S, Akermark B (1997) J Am Chem Soc 119: 6996
7. Ballardini R, Balzani V, Credi A, Gandolfi MT, Venturi M (2001) Acc Chem Res 34: 445
8. (a) Feher G, Allen JP, Yeats TO, Chirino A, Rees DC, Komiya H (1988) Proc Natl Acad Sci USA 85: 7993; (b) Feher G, Allen JP, Yeats TO, Chirino A, Rees DC, Komiya H (1988) Proc Natl Acad Sci USA 85: 8487; (c) Elmer U, Fritzsch G, Buchanan SK, Michel H (1994) Structure 2: 925
9. Nar H, Messerschmidt A, Huber R, van de Kamp M, Canters GW (1991) J Mol Biol 221: 765
10. Inoue T, Sugawara H, Hamanaka S, Tsukui H, Suzuki E, Kohzuma T, Kai Y (1999) Biochemistry 38: 6063
11. (a) Tsukihara T, Aoyama H, Yamashita E, Tomizaki T, Yamaguchi H, Shinzawa-Itoh K, Nakashima R, Yaono R, Yoshikawa S (1996) Science 272: 1136; (b) Tsukihara T, Yamashita E, Tomizaki T, Yamaguchi H, Shinzawa-Itoh K, Nakashima R, Yaono R, Yoshikawa S, Yao M, Inoue N, Mizushima T, Fei MJ, Libeu CP (1998) Science 280: 1723
12. Higuchi Y, Yagi T, Yasouka N (1997) Structure 5: 1671
13. Siegbahn PEM, Blomberg MR, Crabtree RH (1997) Theor Chem Acc 97: 289
14. Jackman MP, McGinnis J, Powls R, Salmon GA (1988) J Am Chem Soc 110: 5880
15. Jackman MP, Lim MC, Sykes AG, Salmon GA (1988) J Chem Soc Dalton Trans 2843
16. Yocom KM et al. (1982) Proc Natl Acad Sci USA 79: 7052
17. (a) Peluso A, Di Donato M, Saracino GAA (2000) J Chem Phys 113: 3212; (b) Peluso A, Di Donato M, Improta R (2000) J Theor Biol 207: 101
18. Beher J, Michel H, Mantele W, Hellwig P (2000) Biochemistry 39: 1356
19. Winkler JR, Nocera DG, Yocom KM, Bordignon E, Gray HB (1982) J Am Chem Soc 104: 5798
20. Isied SS, Worosila G, Atherton SJ (1982) J Am Chem Soc 104: 7659
21. Bechtold R, Kuehn C, Lepre C, Isied SS (1986) Nature 322: 286
22. (a) Therien MJ, Selamn MA, Gray HB, Chang IJ, Winkler JR (1990) J Am Chem Soc 112: 2420; (b) Winkler JR, Gray HB (1992) Chem Rev 92: 369
23. Elias H, Chou MH, Winkler JR (1988) J Am Chem Soc 110: 429
24. Chang I-J, Gray HB, Winkler JR (1991) J Am Chem Soc 113: 7056
25. Louie GV, Bayer GD (1990) J Mol Biol 214: 527
26. Frisch MJ, Trucks GW, Schlegel HB, Gill PMW, Johnson BG, Robb MA, Cheeseman JR, Keith T, Petersson GA, Montgomery JA, Raghavachari K, Al-Laham MA, Zakrzewski VG, Ortiz JV, Foresman JB, Cioslowski J, Stefanov BB, Nanayakkara A, Challacombe M, Peng CY, Ayala PY, Chen W, Wong MW, Andres JL, Replogle ES, Gomperts R, Martin RL, Fox DJ, Binkley JS, Defrees DJ, Baker J, Stewart JP, Head-Gordon M, Gonzalez C, Pople JA (1995) Gaussian 94, revision D.4. Gaussian, Pittsburgh, PA
27. LaChance-Galang KJ, Doan P, Clarke MJ, Rao U, Ymano A, Hoffman BM (1995) J Am Chem Soc 117: 3529
28. Clarke MJ, Bailey VM, Doan PE, Hiller CD, Clarke KJ, LaChance-Galang KJ, Deghilan H, Mandal S, Bastos CM, Lang D (1996) Inorg Chem 35: 4896
29. Krogh-Jespersen K, Westbrook JD, Potenza JA, Schugar HJ (1987) J Am Chem Soc 109: 7025
30. Sundberg RJ, Bryan RF, Taylor IF, Taube H (1974) J Am Chem Soc 96: 381
31. Tomasi J, Persico M (1994) Chem Rev 94: 2027
32. Shin YK, Brunschwig BS, Creutz C, Newton MD, Sutin N (1996) J Phys Chem 100: 1104
33. Delahay P (1984) In: Brundle CR, Backer AD (eds) Electron spectroscopy: theory, techniques and applications. Academic, London, pp 123–196
34. Del Re G, Brahimi M, Peluso A (1999) Chem Phys Lett 299: 511
35. (a) Werner HJ, Knowles PJ (1988) J Chem Phys 89: 5083; (b) Knowles PJ, Werner HJ (1988) Chem Phys Lett 145: 514
36. Jamorski C, Casida ME, Salahub DR (1996) J Chem Phys 104: 5134
37. Schmidt MW, Baldridge KK, Boats JA, Elbert TS, Gordon MS, Jensen JJ, Koseki S, Matsunaga M, Nguyen KA, Su S, Windus TL, Dupuis M, Montgomery JA (1993) J Comput Chem 14: 1347
38. Peluso A, Brahimi M, Carotenuto M, Del Re G (1998) J Phys Chem A 102: 10333
39. (a) Marcus RA (1956) J Chem Phys 24: 966; (b) McConnell HM (1961) J Chem Phys 35: 5008
40. Page CC, Moser CC, Chen X, Dutton PL (1999) Nature 402: 47
41. Peluso A, Di Donato M, Villani G, J phys chem B, in press
42. Perkin MJ (1994) Radical Chemistry. Horwood, London
43. Roth JP, Lovell S, Mayer JM (2000) J Am Chem Soc 122: 5486